

Evaluation of Weather Parameters for Renewable Energy Forecasting with Echo State Networks

Samuel G. Dotson^{a,*}, Kathryn D. Huff^a

^a*Dept. of Nuclear, Plasma, and Radiological Engineering, University of Illinois at Urbana-Champaign, Urbana, IL 61801*

Abstract

Calls for decarbonization led to rapid growth of solar photovoltaic cells and wind turbines. These energy sources vary based on weather features such as solar irradiance and wind speed. This variability challenges grid operators to reliably meet demand through scheduling dispatchable resources. Weather and energy data from the diverse microgrid at the University of Illinois at Urbana-Champaign are used to develop accurate forecasts for total electricity demand, wind power, and solar power with echo state networks. The influence of various weather parameters on forecast accuracy are evaluated. Simulation results show that forecasts can be significantly improved by some additional predictors. These improvements are comparable to the accuracy of more sophisticated algorithms.

Keywords: renewable energy, forecasting, machine learning, echo state networks, grid planning

1. Introduction

1.1. Motivation

In response to the rising threat of climate change, many countries have prioritized reducing carbon emissions. The 2015 Paris Agreement aims to
5 prevent the global temperature from rising more than 1.5 °C above pre-industrial levels [1]. Virtually all current plans to reduce carbon emissions depend on

*Corresponding Author
Email address: sgd2@illinois.edu (Samuel G. Dotson)

increasing the share of energy production by renewable and clean energy sources,
 especially solar and wind [2, 3, 4, 5]. While solar and wind generate zero carbon
 emissions, these forms of electricity generation increase variability, which can lead
 10 to blackouts and power system failures [6]. Further, even modest variable energy
 penetration negatively affects the economics of other clean energy sources, such as
 nuclear power [2, 7, 8]. This may force nuclear plants to shut down prematurely,
 at the precise moment that all clean sources of energy are most needed. Some
 existing work quantified the economic benefit of improving renewable energy
 15 forecasts [9, 10, 11]. Improving renewable energy forecasts can mitigate some of
 the negative side effects of variability. The economic benefits of better forecasts
 include: reduced costs compared to building storage devices [9]; curtailment
 reduction and more efficient use of non-renewable sources [10]; and modest
 load-following from nuclear and biomass generators, which are unable to follow
 20 rapid changes in demand [11]. Most proposed forecasting improvements involve
 new algorithms or machine learning techniques. However, one of the simplest
 approaches to improving forecasts is to improve the training data for such
 algorithms. There is a veritable zoo of weather parameters that can supplement
 target training data, but we don't know *a priori* which of these parameters will
 25 be helpful or detrimental to model performance. In this paper, we evaluate
 several common parameters for use in renewable energy forecasting with Echo
 State Networks (ESNs).

1.2. Why Echo State Networks

ESNs have several appealing features. Simplicity, consisting only of a large,
 30 sparse, reservoir and a single output layer [12]; flexibility and generalizability,
 while other network architectures require significant fine tuning [13]; and speed,
 due to their simple structure and few trainable weights relative to other neural
 networks. The ESN network architecture eliminates the need for complicated
 data pre-processing, such as feature extraction, that is required for other machine
 35 learning and statistical algorithms [14, 15]. ESNs can also outperform other
 prediction techniques [16, 17, 18, 19, 20].

Classical ESNs have previously been used to forecast demand, wind energy, and solar energy [21, 17, 20]. Typically, ESNs make extreme short term predictions, on the order of seconds or minutes [22, 23, 19], one-hour ahead [18], and
40 up to a single day ahead [21]. Forecasts must be multiple-hours to a couple of days ahead to aid unit commitment and grid-scale energy economy [9, 10, 11]. In this work we use a classic ESN architecture to forecast total demand, wind production, and solar production, 4-hours and 48- hours ahead.

Approaches in the literature to improve the forecasting capability of the basic
45 ESN include: adding multiple reservoirs [20, 24, 25, 26], including non-linear units [27, 19], combining with other network architecture [22, 28]; and using a particle swarm approach [29, 23]. Some works indicate that including weather parameters may be useful for renewable energy forecasting [30, 19], but none have demonstrated the effect each parameter has on model performance. The
50 primary goal of this work is filling that gap.

1.3. Contributions

In this work, we use ESNs for three main prediction tasks: total electricity demand, wind energy production, and solar energy production. We split these tasks into further sub tasks, predicting 4-hours ahead and 48-hours ahead. These
55 predictions facilitate scheduling and grid planning because current market rules put renewable energy on the grid first, forcing conventional power generators to work around this variability [9]. Using ESNs to make predictions two-days ahead is unique to this paper since the longest predictions by ESNs in the literature only reach one-day ahead [21]. Finally, we repeat these tasks with several commonly
60 used weather parameters and evaluate their effect on model performance. The need to consider exogenous meteorological inputs has been noted previously. Suprisingly, sun elevation is seldom used as a correlated quantity for energy demand and wind power.

In Section 2 of this paper, we discuss how data were selected and processed, and we review ESNs. Section 3 shows a benchmarking exercise for our ESN
65 implementation and presents the results. We discuss the results and future

implications in Section 4.

2. Methodology

2.1. Echo State Networks

70 An ESN, sometimes called a “reservoir computer,” [31, 32, 33] is a type of recurrent neural network [34] that replaces the many hidden layers of a conventional feed-forward neural network with a reservoir that is:

1. sparse,
2. connected by uniformly random weights, centered at zero,
- 75 3. and large (i.e. has many neurons).

The reservoir is therefore a randomly instantiated adjacency matrix, \mathbf{W} , of size $N \times N$. An input matrix W^{in} , of size $N \times K$, maps the input vector, $U(t)$ with K units, onto the reservoir. The activation states of the reservoir are calculated by [18, 32, 12]

$$x(t) = \tanh(W^{in} \cdot U(t) + \mathbf{W}x(t-1)) \quad (1)$$

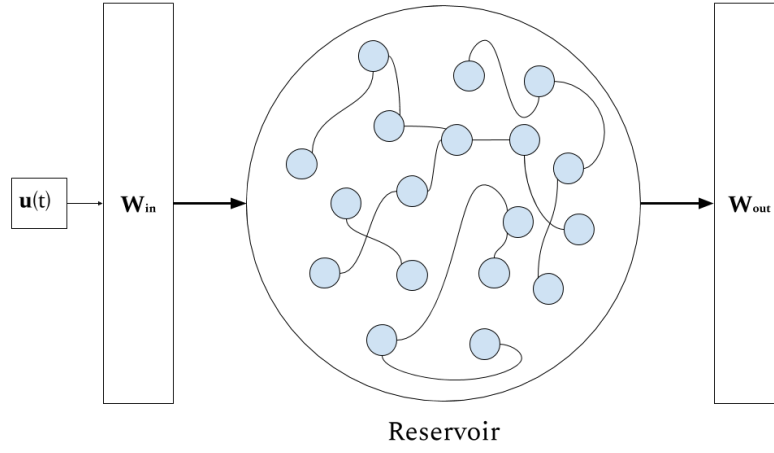
where

$$x(t) = \text{the collection of reservoir activations.}$$

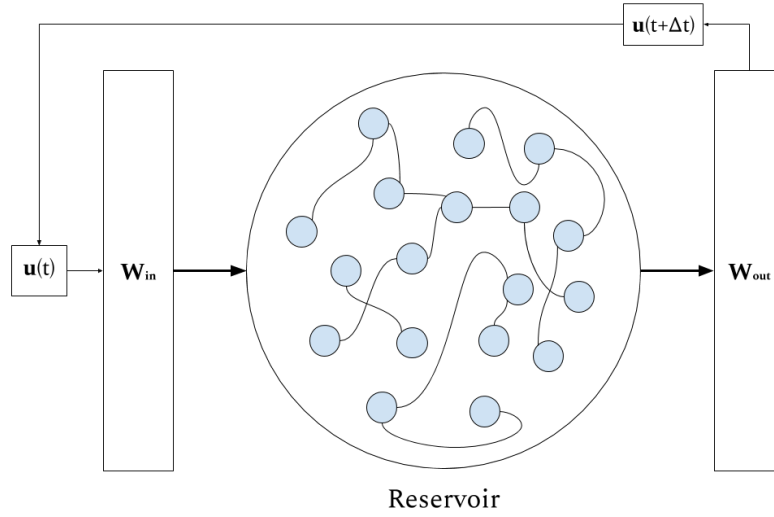
The output is read by an output weight matrix, W^{out} .

$$U(t + \Delta t) = (W^{out})^T \cdot x(t). \quad (2)$$

In the training phase, we discard the output, $U(t + \Delta t)$, and the next training input is passed to the network. During the prediction phase, we keep the output and use it as the next input. Figure 1 illustrates this behavior. The speed of ESNs is owed to this structure – only W^{out} has tunable weights. Everything else
80 is fixed. In this work, we adapted the open source Python package `pyESN` [35] to construct and train the network.



(a) Training Flow



(b) Predicting Flow

Figure 1: (a) Shows the behavior of an ESN during the training phase. (b) Shows ESN behavior during the predicting phase. The output $u(t + \Delta t)$ is used as the next input value.

2.2. Hyper-Parameter Optimization

ESNs are fast because a large reservoir, that does not require training, replaces the hidden layers in a conventional feed-forward neural network. The trade off is that ESNs are sensitive to various hyper-parameters that must be optimized [12]. Table 1 summarizes these hyper-parameters. The spectral radius (ρ) should satisfy the “echo state property” which means that previous reservoir activations have a decaying influence on future states. This is usually guaranteed for $\rho < 1$, but is not a requirement [12].

Table 1: Description of Model Hyper-Parameters

Hyper-parameter	Purpose	Tested Values
noise	Neuron regularization	[0.0001, 0.0003, 0.0007, 0.001, 0.003, 0.005, 0.007, 0.01]
ρ	Spectral radius	[0.5, 0.7, 0.9, 1, 1.1, 1.2, 1.3, 1.5]
N	Size of reservoir, \mathbf{W}	[600, 800, 1000, 1500, 2000, 2500, 3000, 4000]
sparsity	The density of connections in \mathbf{W}	[0.005, 0.01, 0.03, 0.05, 0.1, 0.12, 0.15, 0.2]
Training Length	Size of the training set before prediction	$L \in [5000, 25000]$, step size = 300

We optimize the hyper-parameters by performing a grid search over the test values specified in Table 1. We took the following optimization steps for each prediction task:

1. Select a hyper-parameter or pair of parameters.
2. Generate ESN prediction with the specified parameters.
3. Calculate and record the root mean squared error (RMSE).
4. Continue until last entry in the parameter set is reached.
5. Set the network parameters to hyper-parameter value that minimizes the RMSE.

Figure 2 shows an example heatmap that optimized the spectral radius and
noise hyper-parameters for the 4-hour ahead demand forecast and illustrates the
sensitivity of ESNs to hyperparameter values.

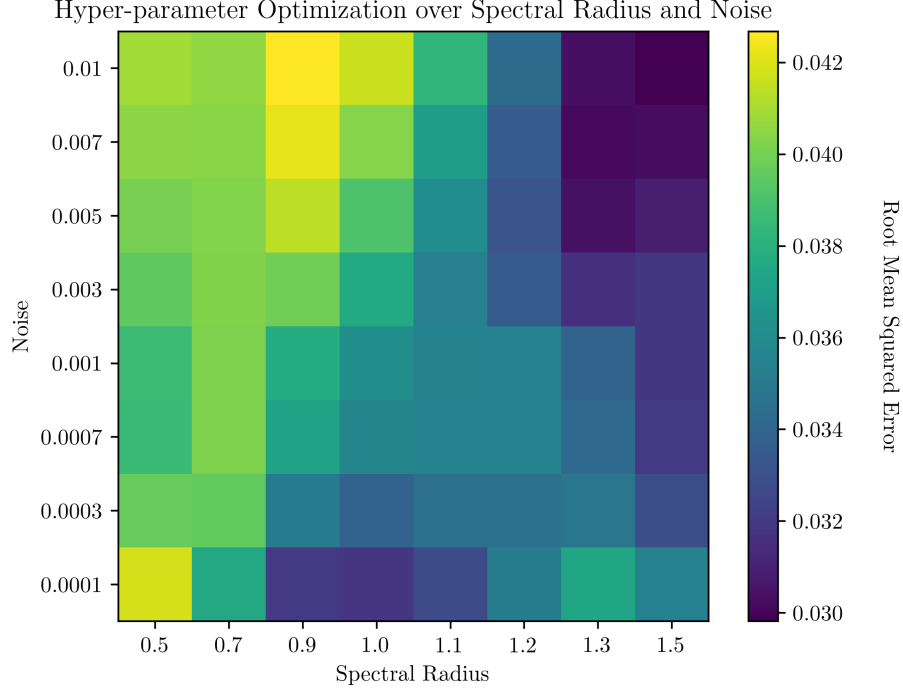


Figure 2: An example heatmap of the RMSE for 4-hour ahead demand prediction with different combinations of spectral radius, ρ , and noise.

2.3. Prediction Tasks

We first performed a benchmarking task by making a prediction for the Lorenz 1963 model [36]. Then, we optimized predictions for univariate time-series representing total demand, solar energy, and wind energy 4-hours ahead
and 48-hours ahead. Finally, we repeated those same six tasks with an additional predictor. Table 2 summarizes each combination of tasks.

Table 2: Summary of prediction tasks.

Target	Future	Additional Predictor
Total Demand	4-hours ahead	None
		Solar Elevation
Solar Energy	48-hours ahead	Humidity
		Pressure
Wind Energy		Wet Bulb Temp.
		Dry Bulb Temp.
		Wind Speed

2.4. Data Selection and Processing

The University of Illinois at Urbana-Champaign (UIUC) Solar Farm 1.0
110 dashboard provides data for the solar energy on campus [37]. The UIUC
Facilities and Services Department shared proprietary data for campus electricity
demand and wind energy with us. All data had hourly resolution. Weather
data were retrieved from the National Oceanic and Atmospheric Administration
(NOAA)[38] for two locations: Champaign, IL, where UIUC is located, and
115 Lincoln, IL, where Railsplitter Windfarm is located. UIUC has a power purchase
agreement with Railsplitter Windfarm [39].

In the case of UIUC solar data, significant portions were missing due to
instrument failure. In order to fill in this missing data, we calculated the
theoretical solar energy production based on irradiance data from OpenEI
[40, 41] with

$$P = G_T \eta_{ref} \tau_{pv} A [1 - \gamma (T - 25)] \quad [W] \quad (3)$$

where

$$G_T = P_{DNI} \cos(\beta + \delta - lat) \quad (4)$$

$$+ P_{DHI} \left(\frac{180 - \beta}{180} \right) \left[\frac{W}{m^2} \right]$$

and

$$\delta = 23.44 \sin \left(\left(\frac{\pi}{180} \right) \left(\frac{360}{365} \right) (N + 284) \right) [^\circ] \quad (5)$$

η, τ, γ = solar panel properties

P_{DNI} = direct normal irradiance

P_{DHI} = diffuse horizontal irradiance

β = tilt angle of the solar panels.

We also calculated the solar elevation angle, α , using coordinates for the UIUC Solar Farm 1.0 [42, 43].

$$\alpha = \sin^{-1} [\sin(\delta) \sin(\phi) + \cos(\delta) \cos(\phi) \cos(\omega)] [^\circ] \quad (6)$$

where

δ = declination angle

ϕ = latitude of interest

ω = hour angle

Finally, we normalized all of the data using the infinity norm

$$\|\mathbf{x}\|_\infty \equiv \max |x_i|. \quad (7)$$

The infinity norm is equivalent to normalizing by the system capacity. This simplifies the comparison of our results between tasks whose training data have vastly different magnitudes. This normalization also makes it possible to compare results with other work and is consistent with the recommendation from Kobylinski et al. (2020) [44]. Table 3 gives the maximum value for each system.

Table 3: Description of the size of the UIUC microgrid

System	Maximum Value
Electricity Load	81.6 [MW]
Solar Energy	4.7 [MW]
Wind Energy	8.8 [MW]

2.5. Performance Metrics

We measure the accuracy of the model using two error metrics: mean absolute error (MAE) and root mean squared error (RMSE). These are defined as

$$\text{MAE} = \frac{1}{N} \sum_{i=1}^N |y_i - \hat{y}_i| \quad (8)$$

$$\text{RMSE} = \sqrt{\frac{1}{N} \sum_{i=1}^N (y_i - \hat{y}_i)^2} \quad (9)$$

where

\hat{y}_i = predicted output

y_i = true value

The MAE measures the expected error throughout the forecast horizon. The RMSE indicates the presence of significant but infrequent errors. Since the data were normalized by system capacity [9], the error metrics are easily interpretable. In order to compare how each individual weather input changed the forecast accuracy, we calculated a “percent improvement” over the univariate case (i.e. a demand prediction based only on historical demand data). This percent improvement is calculated by

$$\% \text{ Improvement} = \frac{\hat{e} - e}{e} \times 100, [-] \quad (10)$$

where

e = error from the univariate forecast

\hat{e} = error from the duovariate forecast.

The sign indicates the direction of change in error. Finally, in order to facilitate comparison with other work, we calculated the normalized root mean squared error (NRMSE) by

$$NRMSE = \sqrt{\frac{\sum_{i=1}^N (y_i - \hat{y}_i)^2}{\sum_{i=1}^N (y_i - \tilde{y})^2}} \quad (11)$$

where

$$\tilde{y} = \text{mean of the target set}$$

3. Results

125 3.1. Benchmark: Lorenz 1963

We first verified that our choice of implementation for a conventional ESN produced similar results to those found in the literature [31]. Table 4 contains the hyper-parameters that minimized the RMSE of the model. Our optimized values differ somewhat from the literature, but our ESN implementation successfully
 130 replicated the climate of the Lorenz Attractor similar to Pathak et. al 2017. Figure 3 shows the ESN forecast ten seconds into the future for Lorenz 1963 model.

Table 4: Hyper-parameters for the Lorenz 1963 model. The random seed was generated by the open source package `numpy`.

Parameter	This paper	Literature [31]
N	2000	300
ρ	0.9	1.2
<code>sparsity</code>	0.1	0.1
<code>noise</code>	0.001	0
Training Length	3200	Not Specified
Random Seed	85	Not Specified

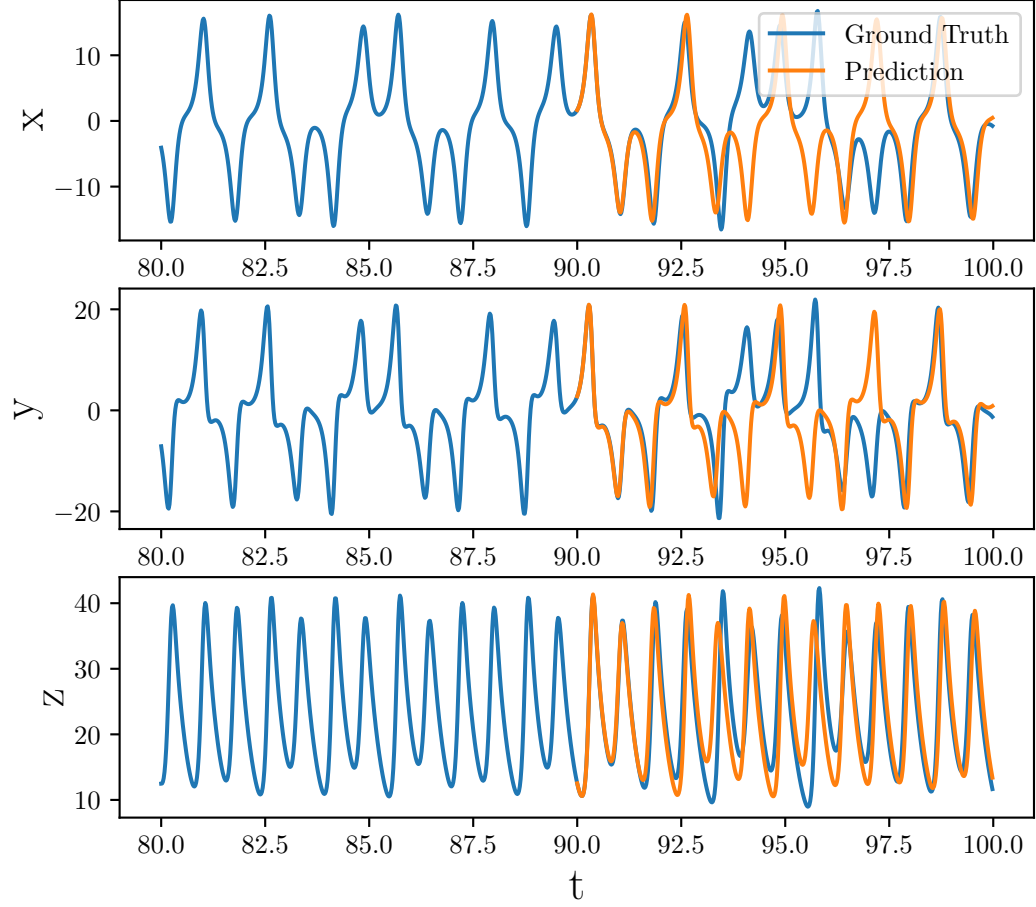


Figure 3: Using an ESN to replicate the climate of the Lorenz Attractor.

3.2. ESN Forecasting: Demand

We used ESNs to forecast electricity demand, or electric load, at both 4-hour
135 intervals and 48-hour intervals. Figure 4 shows the 48-hour ahead forecast that
had the lowest RMSE. In this case, the forecast that used relative humidity as
an additional input had the lowest error, as shown in Table 5. Table 5 also
shows that the forecast was weakened by training with air temperature (both
wet bulb and dry bulb), air pressure, and wind speed. Adding solar elevation
140 angle performed about the same as the base case.

Figure 5 shows the 4-hour interval forecast with the lowest RMSE. Solar elevation angle improved the forecast more than any other meteorological input. Table 6 shows that humidity, air pressure, dry bulb temperature, and wind speed worsened the forecast.

145 This implementation performance is consistent with previous applications of ESNs to the task of predicting electric load [21]. Further, these results indicate that ESNs perform better than other machine learning techniques, long short term memory (LSTM)[45], Sequence to Sequence (S2S) [45], and support vector regression [15], for predicting energy demand.

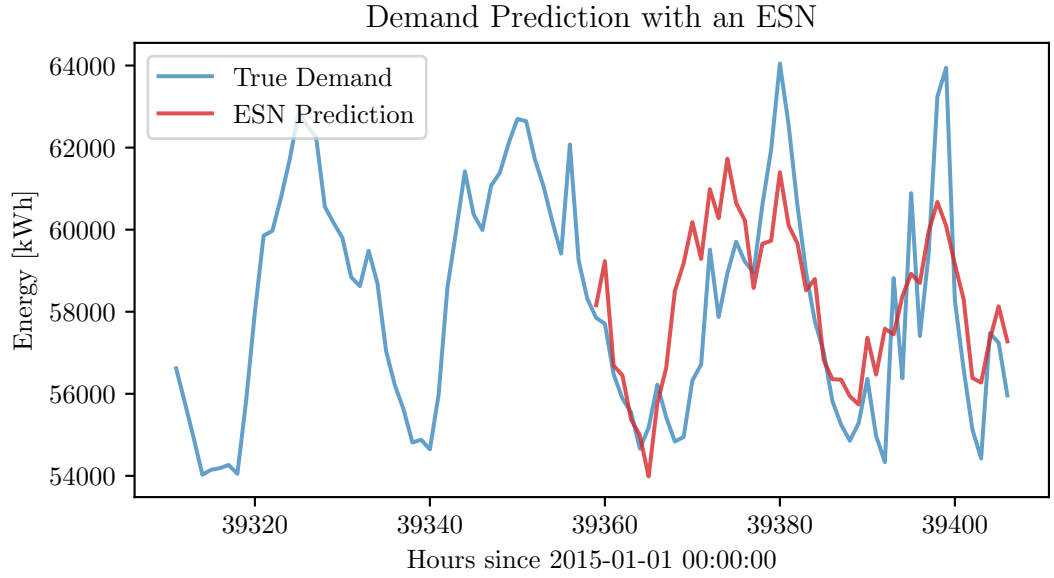


Figure 4: The optimized 48-hour ahead demand prediction. The inputs for this forecast were hourly demand and relative humidity. *Hyperparameters*: Reservoir Size: 1500, Sparsity: 0.2, Spectral Radius: 1.5, Noise: 0.0007, Training Length: 5000, Prediction Window: 48, Random state: 85

Table 5: Tabulated error for 48-hour ahead total electricity demand forecasts with various coupled quantities.

Scenario	NRMSE	MAE	RMSE	Improvement	Improvement
				MAE (%)	RMSE (%)
Total Demand	0.76691	0.0189	0.0241	[-]	[-]
Demand + Sun Elevation	0.76351	0.0191	0.0240	+1.0582	-0.4149
Demand + Humidity	0.70799	0.0180	0.0223	-4.7619	-7.4689
Demand + Pressure	0.77769	0.0176	0.0245	-6.8783	+1.6600
Demand + Wet Bulb Temp.	0.99886	0.0241	0.0314	+27.5132	+30.2904
Demand + Dry Bulb Temp.	0.86634	0.0218	0.0273	+15.3439	+13.2780
Demand + Wind Speed	0.77958	0.0197	0.0245	+4.2328	+1.6600

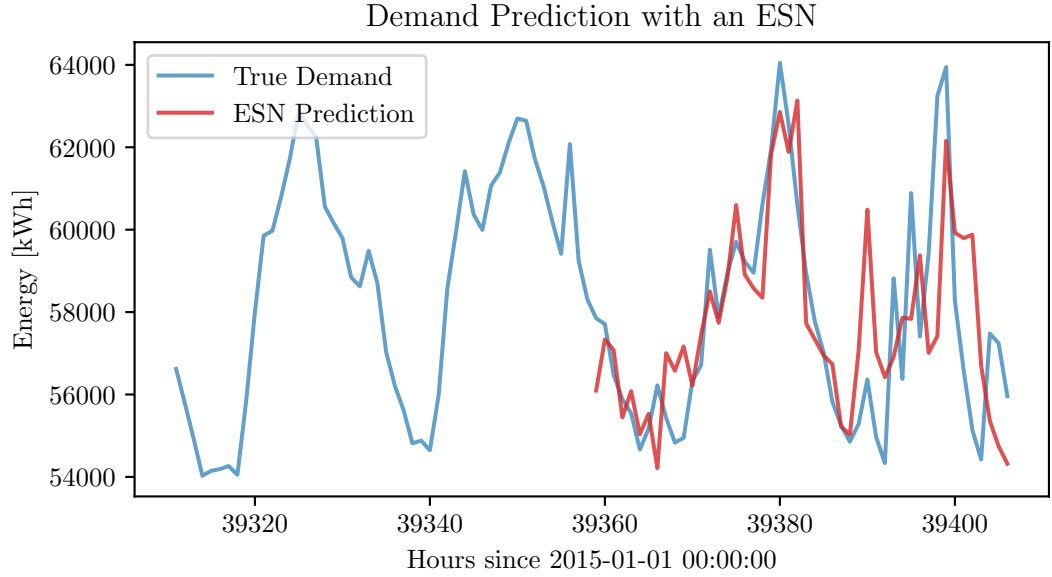


Figure 5: The optimized 4 hour ahead demand prediction. The inputs for this forecast were hourly demand and solar elevation angle. *Hyperparameters*: Reservoir Size: 2500, Sparsity: 0.01, Spectral Radius: 1.5, Noise: 0.003, Training Length: 5000, Prediction Window: 4, Random state: 85.

Table 6: Tabulated error for 4-hour ahead electricity demand forecasts with various coupled quantities.

Scenario	NRMSE	MAE	RMSE	Improvement	Improvement
				MAE (%)	RMSE (%)
Total Demand	0.83634	0.0193	0.0263	[-]	[-]
Demand + Sun Elevation	0.75855	0.0183	0.0239	-5.1831	-9.1255
Demand + Humidity	0.92245	0.0219	0.0290	+13.4715	+10.2662
Demand + Pressure	0.86714	0.0186	0.0273	-3.6269	+3.8023
Demand + Wet Bulb Temp.	0.80366	0.0196	0.0253	+1.5544	-3.8023
Demand + Dry Bulb Temp.	0.85662	0.0208	0.0270	+7.7720	+2.6616
Demand + Wind Speed	0.85152	0.0201	0.0268	+4.1451	+1.9011

150 3.3. ESN Forecasting: Solar Energy

We repeated the 4-hour and 48-hour ahead forecasts for solar energy production on the UIUC campus. Figure 6 and Figure 7 show the best forecasts for 48-hours ahead and 4-hours ahead, respectively. The shaded gray regions emphasize periods when the predicted energy production dipped below zero. This should never occur in reality. Table 7 shows that relative humidity was the best additional feature for the 48-hour ahead prediction, while Table 8 shows that wet bulb temperature improved the forecast the most. In both cases, the predictions were improved by each feature, except for air pressure and wind speed.

160 Our results are comparable to other work that used ESNs to forecast solar energy [30]. However, these results show that conventional ESNs are insufficient for improving energy economics through day-ahead forecasting [11].

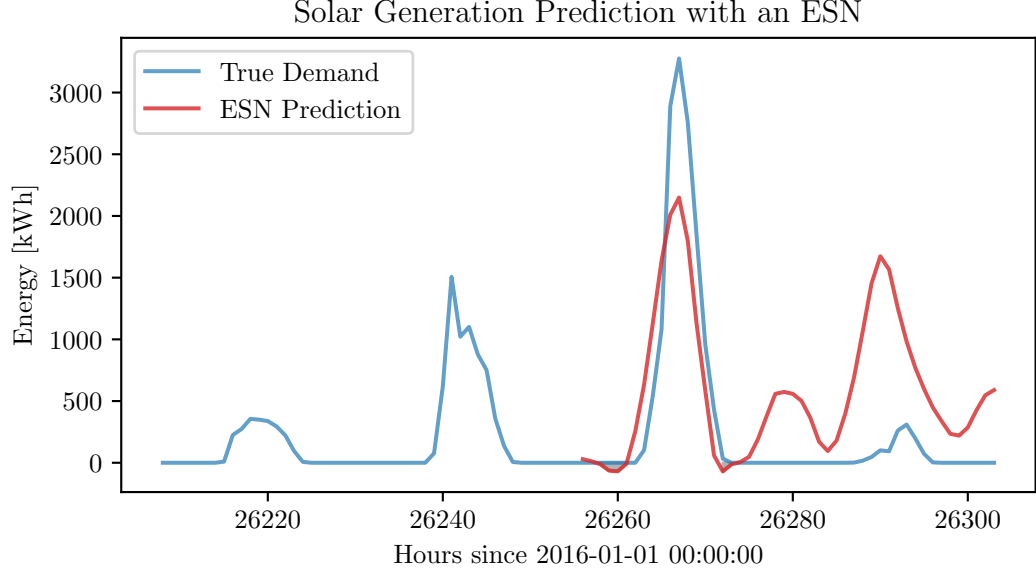


Figure 6: The optimized 48-hour ahead solar energy prediction. The inputs for this forecast were solar energy and relative humidity. Hyperparameters: Reservoir Size: 800, Sparsity: 0.2, Spectral Radius: 1.5, Noise: 0.0001, Training Length: 5000, Prediction Window: 48, Random state: 85

Table 7: Tabulated error for 48-hour ahead solar energy forecasts with various coupled quantities.

Scenario	NRMSE	MAE	RMSE	Improvement	Improvement
				MAE (%)	RMSE (%)
Solar Energy	1.27301	0.1433	0.2062	[-]	[-]
Solar + Sun Elevation	0.84908	0.0957	0.1375	-33.2170	-33.3172
Solar + Humidity	0.80107	0.1001	0.1297	-30.1465	-37.1000
Solar + Pressure	1.33226	0.1910	0.2158	+33.2868	+4.6557
Solar + Wet Bulb Temp.	1.16352	0.1519	0.1884	+6.0014	-8.6324
Solar + Dry Bulb Temp.	0.93376	0.1080	0.1512	-24.6336	-26.6731
Solar + Wind Speed	1.54306	0.2136	0.2500	+49.0579	+21.2415

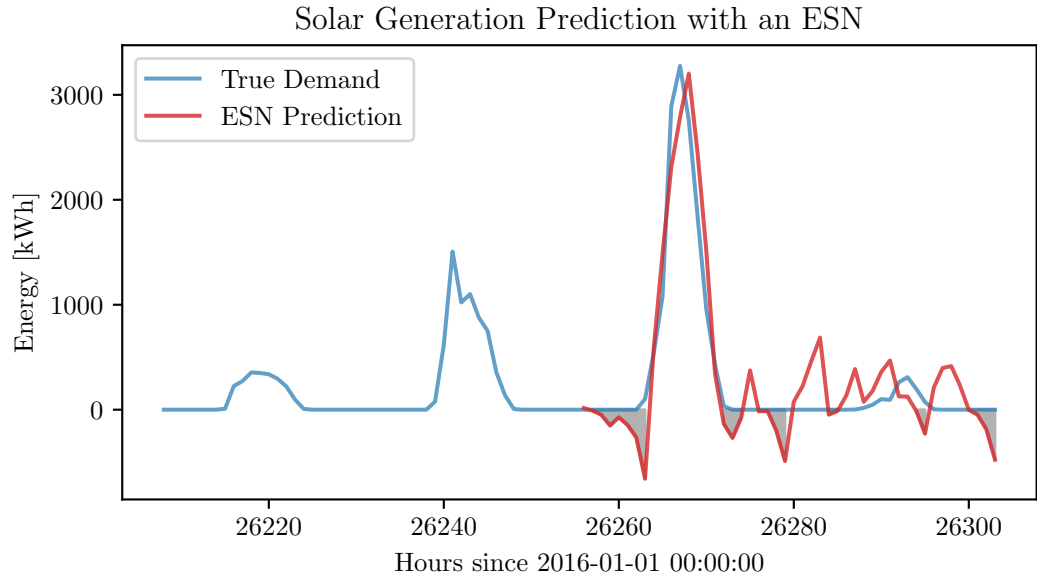


Figure 7: The optimized 4 hour ahead solar energy prediction. The inputs for this forecast were solar energy and hourly wet bulb temperature. *Hyperparameters*: Reservoir Size:800, Sparsity: 0.01, Spectral Radius: 0.9, Noise: 0.0001, Training Length: 5000, Prediction Window: 4, Random state: 85

Table 8: Tabulated error for 4-hour ahead solar energy forecasts with various coupled quantities.

Scenario	NRMSE	MAE	RMSE	Improvement	Improvement
				MAE (%)	RMSE (%)
Solar Energy	0.59151	0.0614	0.0958	[-]	[-]
Solar + Sun Elevation	0.51383	0.0554	0.0832	-9.7720	-13.1524
Solar + Humidity	0.59943	0.0663	0.0971	+7.9804	+1.3570
Solar + Pressure	0.77968	0.0925	0.1263	+50.6515	+31.8372
Solar + Wet Bulb Temp.	0.41541	0.0526	0.0673	-14.3322	-29.7954
Solar + Dry Bulb Temp.	0.61334	0.0682	0.0993	+11.0749	+3.6534
Solar + Wind Speed	0.70216	0.0723	0.1137	+17.7524	+18.6848

3.4. ESN Forecasting: Wind Energy

Finally, we performed the same prediction tasks as before for wind energy. Figure 8 and Figure 9 show the best forecasts that minimized the RMSE for 48- and 4-hours ahead, respectively. All features except air pressure improved the forecast. Including solar elevation angle improved the 48-hour ahead forecast the most, while adding windspeed improved the 4-hour ahead forecast the most. Those results are shown in Table 9 and 10 respectively. Qualitatively, our conventional ESN achieved results comparable to a more complex algorithm by simply adding a single meteorological predictor [28]. Figure 10 shows the results for a 48-hour ahead forecast from a complex hybrid algorithm. Chitsazan et al. 2017 compared wind speed forecasting with a conventional ESN to an ESN with nonlinear readouts and achieved better results with the base model than we did [46]. However, this could be attributed to the fact that they used data with 10-minute resolution and 10-minute prediction steps. Unfortunately they did not include information about the hyper-parameters used for each prediction task.

Still, the state-of-the-art Weather Research and Forecasting model [47], a numerical weather prediction model, far outperforms our best results. Thus, conventional ESNs are insufficient for applications in grid planning [9].

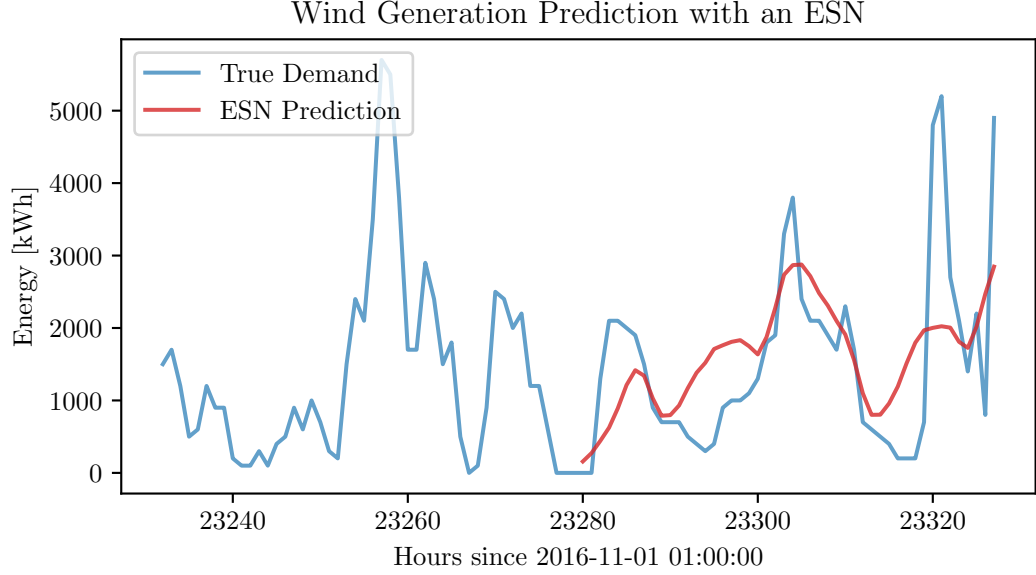


Figure 8: The optimized 48-hour ahead wind energy prediction that minimized the RMSE. The inputs for this forecast were wind energy and solar elevation angle. *Hyperparameters:* Reservoir Size:1000, Sparsity: 0.1, Spectral Radius: 0.9, Noise: 0.0001, Training Length: 19100, Prediction Window: 48, Random state: 85

Table 9: Tabulated error for 48-hour ahead wind forecasts with various coupled quantities.

Scenario	NRMSE	MAE	RMSE	Improvement	Improvement
				MAE (%)	RMSE (%)
Wind Energy	0.93167	0.1035	0.1308	[-]	[-]
Wind + Sun Elevation	0.81220	0.0857	0.1141	-17.1981	-12.7676
Wind + Humidity	0.84950	0.0952	0.1193	-8.0193	-8.7620
Wind + Pressure	0.98345	0.1076	0.1381	+3.9614	+5.5810
Wind + Wet Bulb Temp.	0.84323	0.0886	0.1184	-14.3961	-9.4801
Wind + Dry Bulb Temp.	0.86365	0.0815	0.1213	-21.2560	-7.2630
Wind + Wind Speed	0.84180	0.0763	0.1182	-26.2802	-9.6330

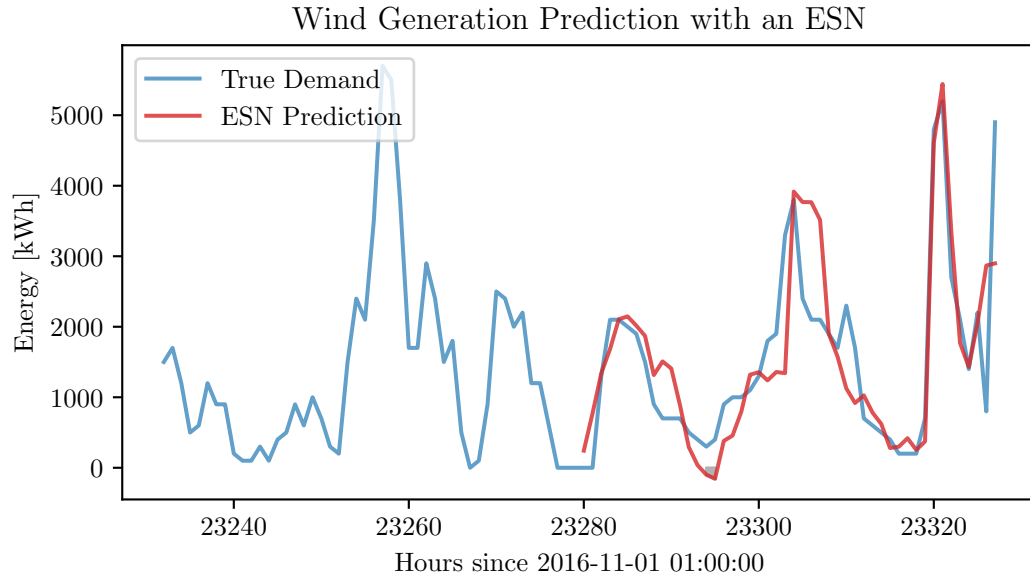


Figure 9: The optimized 4 hour ahead wind energy prediction. The inputs for this forecast were wind energy and hourly windspeed. *Hyperparameters*: Reservoir Size:1000, Sparsity: 0.15, Spectral Radius: 0.9, Noise: 0.001, Training Length: 14300, Prediction Window: 4, Random state: 85

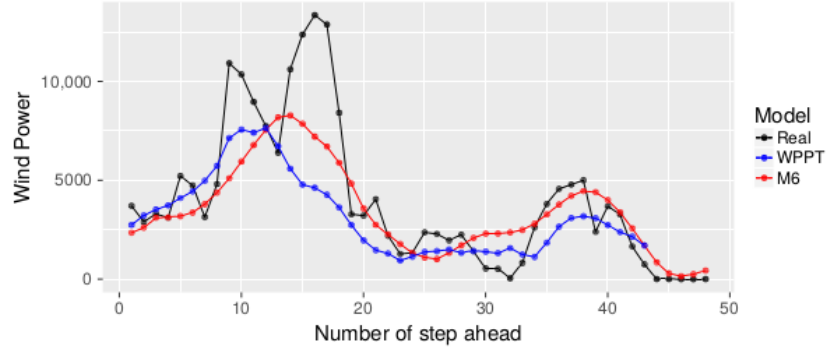


Figure 9. Forecasting using subseries $r = 1$.

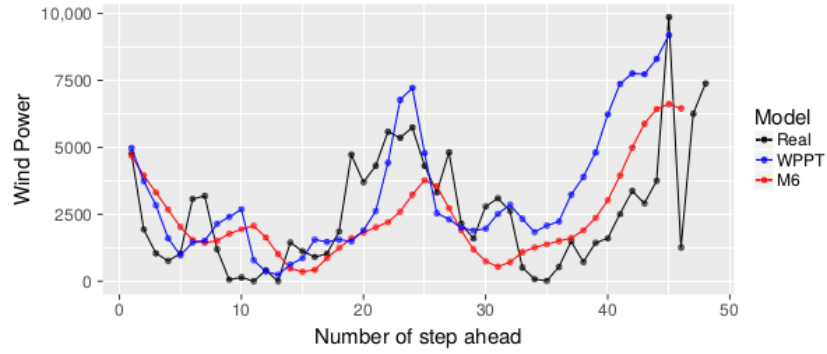
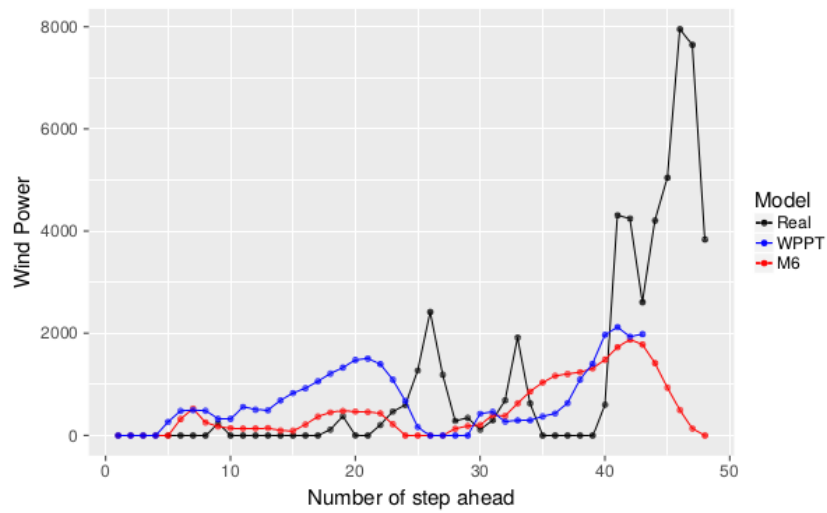


Figure 10. Forecasting using subseries $r = 5$.



21

Figure 11. Forecasting using subseries $r = 10$.

Figure 10: The results of 48-hour ahead predictions from a forecasting algorithm combining ESN and long short term memory algorithms (“M6”). Compared to the Wind Power Prediction Tool (WPPT). Figure reproduced from López et al. 2018 [28].

Table 10: Tabulated error for 4-hour ahead wind forecasts with various coupled quantities.

Scenario	NRMSE	MAE	RMSE	Improvement	Improvement
				MAE (%)	RMSE (%)
Wind Energy	0.88507	0.0903	0.1243	[-]	[-]
Wind + Sun Elevation	0.83394	0.0705	0.1171	-21.9269	-5.7924
Wind + Humidity	0.85522	0.0813	0.1201	-9.9668	-3.3789
Wind + Pressure	0.88587	0.0866	0.1244	-4.0974	+0.0804
Wind + Wet Bulb Temp.	0.76203	0.0731	0.1070	-19.0476	-13.9179
Wind + Dry Bulb Temp.	0.79939	0.0747	0.1123	-17.2757	-9.9654
Wind + Wind Speed	0.59596	0.0571	0.0837	-36.7663	-32.6629

4. Discussion

The forecast accuracy of our ESN for the Lorenz model does not persist for quite as long as in other work [31]. However, our model successfully replicates the environment that produces the Lorenz Attractor. Further, each randomly
185 instantiated reservoir has a unique set of optimal hyper-parameters. It is impossible to replicate the exact conditions of other works without information about a seed for the random state. We have included this information for future work to compare with our results.

For each target variable (demand, wind, and solar) we found that sun ele-
190 vation angle, while not always the best, improved the forecast error in every case. We hypothesize that additional weather features effect model performance due to their temporal complexity relative to the target variable. Electricity demand, for example, is quite “predictable,” and therefore has low complexity. Meanwhile, air temperature and other weather related variables are less pre-
195 dictable. Thus, adding air temperature as a model input increases the total system complexity and weakens performance. Further, solar elevation angle is completely deterministic, perfectly predictable, and either improved, or neutrally effected, model performance in every case. Like electricity demand, solar elevation angle has both diurnal and annual periodicity but has lower complexity than

200 air temperature and electricity demand itself. Conversely, solar and wind energy are both nonlinear functions of many weather variables and consequently have greater complexity than air temperature. This means that adding a temperature feature as a model input will likely decrease the total system complexity and improve the renewable energy forecasts. Including wind speed only improved
 205 the wind energy forecasts, likely because it has greater complexity than solar energy but less than wind energy. Relative humidity has an inconsistent and poorly understood effect on model performance. It improved the forecast for 48-hour ahead electricity demand but worsened it for the 4-hour ahead forecast, as shown in Table 5 and Table 6. The opposite trend occurred for solar energy.
 210 Quantifying the predictability and complexity of these systems is in progress. *Weighted permutation entropy* is a good measure for this type of complexity [48, 49, 50].

These results point to an important disadvantage of using ESNs to forecast renewable energy: Although simple and fast, ESNs remain a black box. We
 215 assume that there exists some underlying dynamics that can be “learned,” but we cannot observe the learning process nor extract important features from ESNs.

We decided the forecast lengths based on the requirements for improved economics and planning mentioned in the literature [9, 10, 11]. The ESN model
 220 performed reasonably well at predicting 4-hours ahead but did not improve on the state-of-the-art [9, 47]. The model did not perform well at the 48-hour ahead forecasts, potentially due to the lack of higher resolution data. ESNs are able to predict highly non-linear systems [51, 34], yet using hourly data could add spurious complexity that confounds the model [49]

225 4.1. Future Work

One appealing avenue of continued work is to leverage ESNs to generate synthetic data that respects real dynamics. Synthetic data are often useful for other machine learning or optimization algorithms. Typically, these data are produced by sampling from an Auto-Regressive Moving Average (ARMA)

230 model [52, 53], which tacitly assumes the training data can be made stationary.
ESNs can replicate the environment of a dynamical system, although it remains
unclear how far in the future this behavior persists [31, 32]. Future work will also
explore the effect of data resolution on model performance, as well as evaluate
improvements to the ESN algorithm.

235 5. Conclusion

Improving renewable energy forecasting is important for grid-planning and
unit commitment, especially as the share of variable renewable resources increases,
challenging the baseload power from nuclear plants. We first demonstrated that
our implementation of the ESN algorithm is consistent with the literature. Then,
240 we used this model to predict total demand, solar energy, and wind energy, and
evaluated the influence of several meteorological factors on model performance.
Our results show that researchers must carefully choose each additional input to
avoid increasing the system complexity. The conventional ESN used here did
not demonstrate an improvement over the state-of-the-art, nor was it accurate
245 enough to improve grid-scale energy economy. Future work will explore other
applications of ESNs and evaluate improvements to the model algorithm.

6. Acknowledgments

This work was made possible with the support from the people at UIUC
Facilities & Services. In particular, Morgan White, Mike Marquissee, and Mike
250 Larson. It was also aided by other members of the Advanced Reactors and Fuel
Cycles (ARFC) group, in particular Nathan Ryan, Nataly Panczyk, and Gavin
Davis. This work is supported by the Nuclear Regulatory Commission Fellowship
Program. Prof. Huff is supported by the Nuclear Regulatory Commission Faculty
Development Program (award NRC-HQ-84-14-G-0054 Program B), the Blue
255 Waters sustained-petascale computing project supported by the National Science
Foundation (awards OCI-0725070 and ACI-1238993) and the state of Illinois,

the DOE ARPA-E MEITNER Program (award DE-AR0000983), and the DOE H2@Scale Program (Award Number: DE-EE0008832)

References

- 260 [1] The paris agreement | UNFCCC.
URL [https://unfccc.int/process-and-meetings/
the-paris-agreement/the-paris-agreement](https://unfccc.int/process-and-meetings/the-paris-agreement/the-paris-agreement)
- [2] C. Cany, C. Mansilla, G. Mathonnière, P. da Costa, Nuclear contribution
to the penetration of variable renewable energy sources in a french decar-
265 bonised power mix 150 544–555. doi:10.1016/j.energy.2018.02.122.
URL [http://www.sciencedirect.com/science/article/pii/
S0360544218303566](http://www.sciencedirect.com/science/article/pii/S0360544218303566)
- [3] J. Chilvers, T. J. Foxon, S. Galloway, G. P. Hammond, D. Infield, M. Leach,
P. J. Pearson, N. Strachan, G. Strbac, M. Thomson, Realising transition
270 pathways for a more electric, low-carbon energy system in the united
kingdom: Challenges, insights and opportunities 231 (6) 440–477, publisher:
IMECHE. doi:10.1177/0957650917695448.
URL <https://doi.org/10.1177/0957650917695448>
- [4] 99th General Assembly, Illinois general assembly - full text of SB2814.
275 URL [http://www.ilga.gov/legislation/fulltext.asp?DocName=
&SessionId=88&GA=99&DocTypeId=SB&DocNum=2814&GAID=13&LegID=
96125&SpecSess=&Session=](http://www.ilga.gov/legislation/fulltext.asp?DocName=&SessionId=88&GA=99&DocTypeId=SB&DocNum=2814&GAID=13&LegID=96125&SpecSess=&Session=)
- [5] iSEE, Illinois climate action plan (iCAP).
- [6] H. Haes Alhelou, M. E. Hamedani-Golshan, T. C. Njenda, P. Siano, A survey
280 on power system blackout and cascading events: Research motivations and
challenges 12 (4) 682, number: 4 Publisher: Multidisciplinary Digital
Publishing Institute. doi:10.3390/en12040682.
URL <https://www.mdpi.com/1996-1073/12/4/682>

- [7] J. H. Keppler, C. Marcantonini, O. N. E. Agency, O. for Economic Co-
 285 operation {and} Development, Carbon pricing, power markets and the
 competitiveness of nuclear power, Nuclear development, Nuclear Energy
 Agency, Organisation for Economic Co-operation and Development.
- [8] Illinois Commerce Commision (ICC), I. P. A. (IPA), I. E. P. A. (IEPA),
 I. D. of Commerce and Economic Opportunity (IDCEO), Potential nuclear
 290 power plant closings in illinois.
 URL [http://www.ilga.gov/reports/special/Report_Potential%
 20Nuclear%20Power%20Plant%20Closings%20in%20IL.pdf](http://www.ilga.gov/reports/special/Report_Potential%20Nuclear%20Power%20Plant%20Closings%20in%20IL.pdf)
- [9] Q. Wang, C. B. Martinez-Anido, H. Wu, A. R. Florita, B.-M. Hodge,
 Quantifying the economic and grid reliability impacts of improved wind
 295 power forecasting 7 (4) 1525–1537, conference Name: IEEE Transactions
 on Sustainable Energy. doi:10.1109/TSTE.2016.2560628.
- [10] E. V. Mc Garrigle, P. G. Leahy, Quantifying the value of improved
 wind energy forecasts in a pool-based electricity market 80 517–524.
 doi:10.1016/j.renene.2015.02.023.
 300 URL [http://www.sciencedirect.com/science/article/pii/
 S0960148115001135](http://www.sciencedirect.com/science/article/pii/S0960148115001135)
- [11] C. Brancucci Martinez-Anido, B. Botor, A. R. Florita, C. Draxl, S. Lu, H. F.
 Hamann, B.-M. Hodge, The value of day-ahead solar power forecasting
 improvement 129 192–203. doi:10.1016/j.solener.2016.01.049.
 305 URL [http://www.sciencedirect.com/science/article/pii/
 S0038092X16000736](http://www.sciencedirect.com/science/article/pii/S0038092X16000736)
- [12] M. Lukoševičius, A practical guide to applying echo state networks, in:
 G. Montavon, G. B. Orr, K.-R. Müller (Eds.), Neural Networks: Tricks of
 the Trade: Second Edition, Lecture Notes in Computer Science, Springer,
 310 pp. 659–686. doi:10.1007/978-3-642-35289-8_36.
 URL https://doi.org/10.1007/978-3-642-35289-8_36

- [13] H. Liu, C. Chen, X. Lv, X. Wu, M. Liu, Deterministic wind energy forecasting: A review of intelligent predictors and auxiliary methods 195 328–345, publisher: Pergamon. doi:10.1016/j.enconman.2019.05.020.
 315 URL <http://www.sciencedirect.com/science/article/pii/S0196890419305655>
- [14] D. Lazos, A. B. Sproul, M. Kay, Optimisation of energy management in commercial buildings with weather forecasting inputs: A review 39 587–603. doi:10.1016/j.rser.2014.07.053.
 320 URL <https://www.sciencedirect.com/science/article/pii/S136403211400505X>
- [15] Y. Chen, H. Tan, U. Berardi, Day-ahead prediction of hourly electric demand in non-stationary operated commercial buildings: A clustering-based hybrid approach 148 228–237. doi:10.1016/j.enbuild.2017.05.003.
 325 URL <https://www.sciencedirect.com/science/article/pii/S0378778816313792>
- [16] I. Jayawardene, G. K. Venayagamoorthy, Comparison of echo state network and extreme learning machine for PV power prediction, in: 2014 IEEE Symposium on Computational Intelligence Applications in Smart Grid (CIASG), pp. 1–8, ISSN: 2326-7690. doi:10.1109/CIASG.2014.7011546.
 330 (CIASG), pp. 1–8, ISSN: 2326-7690. doi:10.1109/CIASG.2014.7011546.
- [17] I. Jayawardene, G. Venayagamoorthy, Comparison of adaptive neuro-fuzzy inference systems and echo state networks for PV power prediction 53 92–102. doi:10.1016/j.procs.2015.07.283.
- [18] G. Shi, D. Liu, Q. Wei, Energy consumption prediction of office buildings based on echo state networks 216 478–488. doi:10.1016/j.neucom.2016.08.004.
 335 URL <http://www.sciencedirect.com/science/article/pii/S0925231216308219>
- [19] M. A. Chitsazan, M. S. Fadali, A. Tryznadlowski, Wind speed and wind direction forecasting using echo state network with nonlinear functions 131
 340

879–889, publisher: Pergamon. doi:10.1016/j.renene.2018.07.060.

URL <http://www.sciencedirect.com/science/article/pii/S0960148118308577>

- [20] H. Hu, L. Wang, S.-X. Lv, Forecasting energy consumption and
345 wind power generation using deep echo state network 154 598–613.
doi:10.1016/j.renene.2020.03.042.

URL <http://www.sciencedirect.com/science/article/pii/S0960148120303645>

- [21] A. Deihimi, H. Showkati, Application of echo state networks
350 in short-term electric load forecasting 39 (1) 327–340. doi:
10.1016/j.energy.2012.01.007.

URL <https://linkinghub.elsevier.com/retrieve/pii/S0360544212000126>

- [22] Y. Chen, Z. He, Z. Shang, C. Li, L. Li, M. Xu, A novel combined model
355 based on echo state network for multi-step ahead wind speed forecasting: A
case study of NREL 179 13–29. doi:10.1016/j.enconman.2018.10.068.

URL <https://linkinghub.elsevier.com/retrieve/pii/S0196890418311968>

- [23] H. Wang, Z. Lei, Y. Liu, J. Peng, J. Liu, Echo state network
360 based ensemble approach for wind power forecasting 201 112188.
doi:10.1016/j.enconman.2019.112188.

URL <http://www.sciencedirect.com/science/article/pii/S019689041931194X>

- [24] C. Gallicchio, A. Micheli, Deep echo state network (DeepESN): A brief
365 survey [arXiv:1712.04323](https://arxiv.org/abs/1712.04323).

URL <http://arxiv.org/abs/1712.04323>

- [25] X. Yao, Z. Wang, H. Zhang, A novel photovoltaic power
forecasting model based on echo state network 325 182–189.

doi:10.1016/j.neucom.2018.10.022.

370 URL <http://www.sciencedirect.com/science/article/pii/S0925231218312104>

- [26] Q. Li, Z. Wu, R. Ling, L. Feng, K. Liu, Multi-reservoir echo state computing for solar irradiance prediction: A fast yet efficient deep learning approach 95 106481. doi:10.1016/j.asoc.2020.106481.

375 URL <https://linkinghub.elsevier.com/retrieve/pii/S1568494620304208>

- [27] G. Holzmann, H. Hauser, Echo state networks with filter and a delay&sum readout.

- [28] E. López, C. Valle, H. Allende, E. Gil, H. Madsen, Wind power forecasting based on echo state networks and long short-term memory 11 (3) 526, number: 3 Publisher: Multidisciplinary Digital Publishing Institute. doi: 10.3390/en11030526.

380 URL <https://www.mdpi.com/1996-1073/11/3/526>

- [29] N. Chouikhi, B. Ammar, N. Rokbani, A. M. Alimi, PSO-based analysis of echo state network parameters for time series forecasting 55 211–225. doi:10.1016/j.asoc.2017.01.049.

385 URL <https://linkinghub.elsevier.com/retrieve/pii/S1568494617300649>

- [30] Q. Li, Z. Wu, R. Ling, M. Tan, Echo state network-based spatio-temporal model for solar irradiance estimation 158 3808–3813, publisher: Elsevier. doi:10.1016/j.egypro.2019.01.868.

390 URL <http://www.sciencedirect.com/science/article/pii/S1876610219309105>

- [31] J. Pathak, Z. Lu, B. R. Hunt, M. Girvan, E. Ott, Using machine learning to replicate chaotic attractors and calculate lyapunov exponents from data 27 (12) 121102. arXiv:1710.07313, doi:10.1063/1.5010300.

395 URL <http://arxiv.org/abs/1710.07313>

- [32] J. Pathak, B. Hunt, M. Girvan, Z. Lu, E. Ott, Model-free prediction of large spatiotemporally chaotic systems from data: A reservoir computing approach 120 (2) 024102, publisher: American Physical Society. doi: 10.1103/PhysRevLett.120.024102.
URL <https://link.aps.org/doi/10.1103/PhysRevLett.120.024102>
- [33] P. R. Vlachas, J. Pathak, B. R. Hunt, T. P. Sapsis, M. Girvan, E. Ott, P. Koumoutsakos, Backpropagation algorithms and reservoir computing in recurrent neural networks for the forecasting of complex spatiotemporal dynamics 126 191–217. doi:10.1016/j.neunet.2020.02.016.
URL <http://www.sciencedirect.com/science/article/pii/S0893608020300708>
- [34] M. Lukoševičius, H. Jaeger, Reservoir computing approaches to recurrent neural network training 3 (3) 127–149. doi: 10.1016/j.cosrev.2009.03.005.
URL <http://www.sciencedirect.com/science/article/pii/S1574013709000173>
- [35] C. Korndörfer, pyESN.
URL <https://github.com/cknd/pyESN>
- [36] E. N. Lorenz, Deterministic nonperiodic flow 20 (2) 130–141, publisher: American Meteorological Society Section: Journal of the Atmospheric Sciences. doi:10.1175/1520-0469(1963)020<0130:DNF>2.0.CO;2.
URL https://journals.ametsoc.org/view/journals/atsc/20/2/1520-0469_1963_020_0130_dnf_2_0_co_2.xml
- [37] AlsoEnergy, University of illinois solar farm dashboard, <http://go.illinois.edu/solar>.
URL <http://go.illinois.edu/solar>
- [38] N. C. for Environmental Information, Find a station | data tools | climate data online (CDO) | national climatic data center (NCDC).
URL <https://www.ncdc.noaa.gov/cdo-web/datatools/findstation>

- [39] S. Breitweiser, Wind power: University of illinois at urbana-champaign.
 URL https://www.fs.illinois.edu/docs/default-source/news-docs/newsrelease_windppa___factsheet.pdf?sfvrsn=43aaffea_0
- [40] National solar radiation data base - NSRDB viewer - OpenEI datasets.
 URL <https://openei.org/datasets/dataset/national-solar-radiation-data-base/resource/b2074dd9-36a4-4382-a12f-e795b578404c>
- [41] H. E. Garcia, J. Chen, J. S. Kim, M. G. McKellar, W. R. Deason, R. B. Vilim, S. M. Bragg-Sitton, R. D. Boardman, Nuclear hybrid energy systems regional studies: West texas & northeastern arizona. doi:10.2172/1236837.
- [42] N. US Department of Commerce, ESRL global monitoring laboratory - global radiation and aerosols.
 URL <https://www.esrl.noaa.gov/gmd/grad/solcalc/calcdetails.html>
- [43] J. Meeus, Astronomical Algorithms, 2nd Edition, Willmann-Bell, Inc.
- [44] P. Kobylinski, M. Wierzbowski, K. Piotrowski, High-resolution net load forecasting for micro-neighbourhoods with high penetration of renewable energy sources 117 105635. doi:10.1016/j.ijepes.2019.105635.
 URL <http://www.sciencedirect.com/science/article/pii/S0142061518335257>
- [45] D. L. Marino, K. Amarasinghe, M. Manic, Building energy load forecasting using deep neural networks, in: IECON 2016 - 42nd Annual Conference of the IEEE Industrial Electronics Society, pp. 7046–7051. doi:10.1109/IECON.2016.7793413.
- [46] M. A. Chitsazan, M. S. Fadali, A. K. Nelson, A. M. Trzynadlowski, Wind speed forecasting using an echo state network with nonlinear output func-

- tions, in: 2017 American Control Conference (ACC), pp. 5306–5311, ISSN: 2378-5861. doi:10.23919/ACC.2017.7963779.
- [47] J. G. Powers, J. B. Klemp, W. C. Skamarock, C. A. Davis, J. Dudhia, D. O. Gill, J. L. Coen, D. J. Gochis, R. Ahmadov, S. E. Peckham, G. A. Grell, J. Michalakes, S. Trahan, S. G. Benjamin, C. R. Alexander, G. J. Dimego, W. Wang, C. S. Schwartz, G. S. Romine, Z. Liu, C. Snyder, F. Chen, M. J. Barlage, W. Yu, M. G. Duda, The weather research and forecasting model: Overview, system efforts, and future directions 98 (8) 1717–1737, publisher: American Meteorological Society Section: Bulletin of the American Meteorological Society. doi:10.1175/BAMS-D-15-00308.1. URL <https://journals.ametsoc.org/view/journals/bams/98/8/bams-d-15-00308.1.xml>
- [48] B. Fadlallah, B. Chen, A. Keil, J. Príncipe, Weighted-permutation entropy: A complexity measure for time series incorporating amplitude information 87 (2) 022911, publisher: American Physical Society. doi:10.1103/PhysRevE.87.022911. URL <https://link.aps.org/doi/10.1103/PhysRevE.87.022911>
- [49] J. Garland, R. James, E. Bradley, Model-free quantification of time-series predictability 90 (5) 052910, publisher: American Physical Society. doi:10.1103/PhysRevE.90.052910. URL <https://link.aps.org/doi/10.1103/PhysRevE.90.052910>
- [50] F. Pennekamp, A. C. Iles, J. Garland, G. Brennan, U. Brose, U. Gaedke, U. Jacob, P. Kratina, B. Matthews, S. Munch, M. Novak, G. M. Palamara, B. C. Rall, B. Rosenbaum, A. Tabi, C. Ward, R. Williams, H. Ye, O. L. Petchey, The intrinsic predictability of ecological time series and its potential to guide forecasting 89 (2) e01359, eprint: <https://esajournals.onlinelibrary.wiley.com/doi/pdf/10.1002/ecm.1359>. doi:<https://doi.org/10.1002/ecm.1359>.

URL <https://esajournals.onlinelibrary.wiley.com/doi/abs/10.1002/ecm.1359>

[51] H. Jaeger, Harnessing nonlinearity: Predicting chaotic systems
485 and saving energy in wireless communication 304 (5667) 78–80.
doi:10.1126/science.1091277.

URL <https://www.sciencemag.org/lookup/doi/10.1126/science.1091277>

[52] T. E. Baker, A. S. Epiney, C. Rabiti, E. Shittu, Optimal sizing of flexible
490 nuclear hybrid energy system components considering wind volatility 212
498–508.

[53] H. E. Garcia, J. Chen, J. S. Kim, R. B. Vilim, W. R. Binder, S. M.
Bragg Sitton, R. D. Boardman, M. G. McKellar, C. J. J. Paredis, Dynamic
performance analysis of two regional nuclear hybrid energy systems 107
495 234–258. doi:10.1016/j.energy.2016.03.128.

URL <http://www.sciencedirect.com/science/article/pii/S0360544216303759>